Surface-Emitting Laser—Its Birth and Generation of New Optoelectronics Field

Kenichi Iga, *Fellow, IEEE*

Invited Paper

***Abstract*—The surface-emitting laser (SEL) is considered one of the most important devices for optical interconnects and LANs, enabling ultra parallel information transmission in lightwave and computer systems. In this paper, we will introduce its history, fabrication technology, and discuss the advantages. Then, we review the progress of the surface-emitting laser and the vertical-cavity surface-emitting laser (VCSEL), covering the spectral band from infrared to ultraviolet by featuring its physics, materials, fabrication technology, and performances, such as threshold, output powers, polarizations, line-width, modulation, reliability, and so on.**

***Index Terms*—DBR, distributed Bragg reflector, gigabit ethernet, LAN, laser array, microlaser, microlens, multilayer, parallel transmission, quantum well, semiconductor laser, surface-emitting laser, vertical cavity laser, vertical-cavity surface-emitting laser.**

I. Introduction

WHAT IS THE surface-emitting laser (SEL) or the vertical cavity surface-emitting laser (VCSEL)? The structure is substantially different from conventional stripe lasers, i.e., the vertical cavity is formed by the surfaces of epitaxial layers and light output is taken from one of the mirror surfaces as shown in Fig. 1(a).

VCSEL [1], [2] looked to meet the third generation of development in 1999, as seen from Table I, as we entered a new information and technology era in 2000. The VCSEL is being applied in various optical systems, such as optical networks, parallel optical interconnects, laser printers, high density optical disks, and so on. We review its history and the progress of VCSELs in wide spectral ranges covered by various *III–V* compound semiconductors. Recent technologies and future prospects will be discussed.

We summarized the brief history of VCSEL research in Table I. It is recognized that the author suggested the device of VCSEL in 1977, as shown in Fig. 1(b). The first device came out in 1979, where we used a 1300-nm wavelength GaInAsP–InP material for the active region [3]. In 1986, we made a 6-mA threshold GaAs device [4] and then employed the metal organic chemical vapor deposition (MOCVD). The first room-temperature continuous-wave (CW) device using GaAs material was demonstrated in 1988 [5]. In 1989, Jewell demonstrated a GaInAs VCSEL exhibiting a 1–2-mA threshold [6]. These two experiments encouraged the audience to be getting up at the stage of vertical-cavity surface-emitting laser research. Submilliampere threshold devices were demonstrated

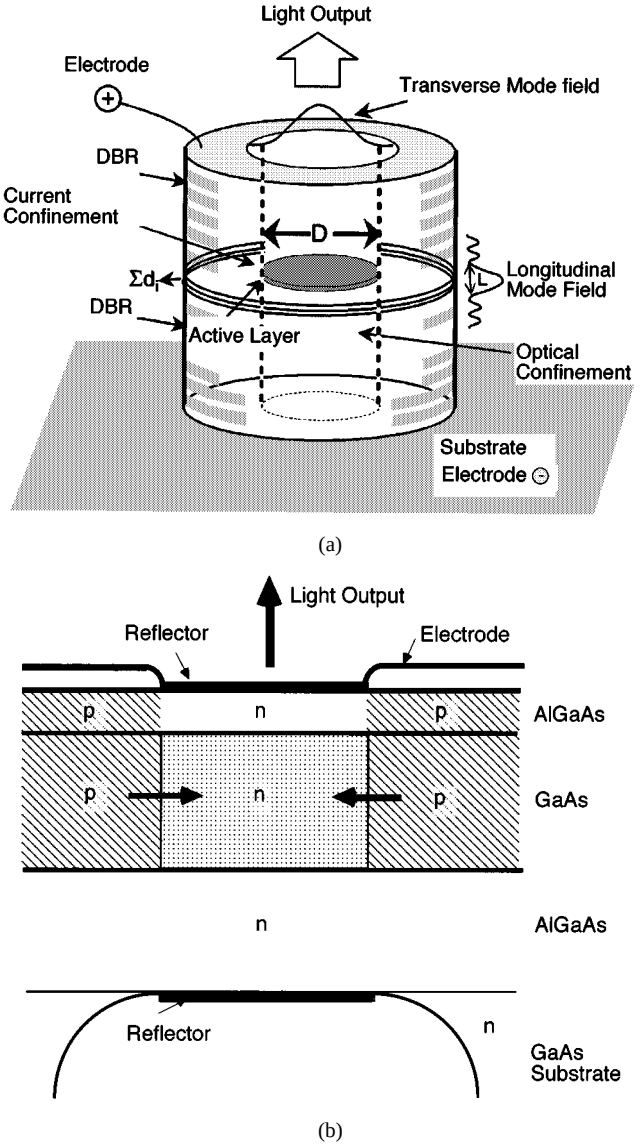

Fig. 1. Model of VCSEL. (a) Current model. (b) Initial idea.

Manuscript received July 13, 2000. This work was supported by the Ministry of Education, Science, Sport, and Culture with a Grant from COE Program 07CE2003.

The author is with the P&I Microsystem Research Center, Tokyo Institute of Technology, 4259 Nagatsuta, Midoriku, Yokohama 226-8503, Japan.

Publisher Item Identifier S 1077-260X(00)11545-X.

TABLE I
HISTORY OF VCSEL RESEARCH

I	1977-	First Idea and Initial Demonstrations
II	1988-	CW and Device Feasibility Study
III	1999-	Production and Extension of Applications

by improving the active region and distributed Bragg reflectors (DBRs).

Since 1992, VCSELs based on GaAs have been extensively studied [7]–[9] and some 780, 850, and 980-nm devices are now commercialized into optical systems. We improved a 1500-nm VCSEL [10] demonstrated a 1300-nm room-temperature CW device [11]. A wafer fusion technique enabled us to operate 1550-nm VCSELs at higher temperatures [12]. In 1993, a room-temperature high-performance CW red AlGaInAs device was demonstrated [13]. Since 1996, green-blue-ultraviolet device research was started [14], [15]. Since 1999, VCSEL-based optical transmitters have been introduced into gigabit per second LANs.

The initial motivation of SEL invention was a fully monolithic fabrication of laser cavity. Based upon this concept, the current issues include high speed modulation capability at very low-power consumption level, reproducible array production, and inexpensive moduling.

The VCSEL structure may provide a number of advantages as follows:

1) ultralow threshold operation is expected from its small cavity volume, reaching microampere levels;
2) $(I - I_{\rm th})I_{\rm th} > 100$ is possible, where I = driving current and $I_{\rm th}$ = threshold current;
3) wavelength and thresholds are relatively insensitive against temperature variation;
4) dynamic single-mode operation is possible;
5) large relaxation frequency provides high-speed modulation capability;
6) long device lifetime is due to completely embedded active region and passivated surfaces;
7) high-power conversion efficiency, i.e., $>50\%$;
8) vertical emission from substrate;
9) easy coupling to optical fibers due to good mode matching from single mode through thick multimode fibers;
10) a number of laser devices can be fabricated by fully monolithic processes yielding very low cost chip production;
11) the initial probe test can be performed before separating devices into discrete chips;
12) easy bonding and mounting;
13) cheap modules and package cost;
14) densely packed and precisely arranged two-dimensional (2-D) laser arrays can be formed;
15) vertical stack integration of multithin-film functional optical devices can be made intact to the VCSEL resonator, taking the advantage of micromachining technology and providing polarization independent characteristics;
16) compatible integration together with LSIs.

In this paper, we would like to review the progress of VCSELs in a wide range of optical spectra based on GaInAsP, AlGaInAs, GaInNAs, GaInAs, GaAlAs, AlGaInP, ZnSe, GaInN, and other materials.

II. BASICS OF VCSEL

A. Threshold Current

The physical difference between VCSELs and conventional stripe geometry lasers is summarized in Table II. The major points are that the cavity length of VCSELs is in the order of wavelength which is much smaller than that of stripe lasers, having about a 300-μm wavelength and several micrometers of lateral size. Those provide us with substantial differences in laser performances.

We would like to discuss the threshold current of VCSELs. The threshold current $I_{\rm th}$ of SELs can be expressed by the equation with threshold current density $J_{\rm th}$

$$I_{\rm th} = \pi(D/2)^2 J_{\rm th} = \frac{{\rm e}VN_{\rm th}}{\eta_i \tau_s} \cong \frac{{\rm e}VB_{\rm eff}}{\eta_i \eta_{\rm spon}} N_{\rm th}^2 \qquad (1)$$

where e is electron charge. V is the volume of active region, which is given by

$$V = \pi(D/2)^2 d. \qquad (2)$$

The threshold carrier density is given by

$$N_{\rm th} = N_t + \frac{\alpha_a + \alpha_d + \alpha_m}{A_0 \xi}. \qquad (3)$$

The parameters used are defined as follows, where

α_a absorption loss coefficient averaged per unit length;
α_d diffraction loss coefficient averaged per unit length;
α_m mirror loss coefficient;
A_0 gain coefficient expressing differential gain $A_0 = dg/dN$, with g as the optical gain per centimeters;
$B_{\rm eff}$ effective recombination coefficient;
d total active layer thickness;
D diameter of active region;
L effective cavity length, including spacing layers and penetration layers of Bragg reflectors;
N_t transparent carrier density;
τ_p photon lifetime in cavity;
τ_s recombination lifetime;
ξ optical energy confinement factor, $\xi = \xi_t \xi_l$;
ξ_t transverse confinement factor;
ξ_l longitudinal confinement factor or filling factor relative to stripe lasers $\xi_l = d/L$ (for thick active layer) $\xi_l = 2d/L$ (for thin active layer, which is located at the loop of optical standing wave);
η_i injection efficiency, sometimes referred as internal efficiency;
$\eta_{\rm spon}$ spontaneous emission efficiency.

As seen in (1), we recognize that it is essential to reduce the volume of active region in order to decrease the threshold current. Assume that the threshold carrier density does not change that much. If we reduce the active volume, we can decrease the threshold as we make a small active region. We compare the dimensions of surface-emitting lasers and conventional stripe ge-

TABLE II
COMPARISON OF PARAMETERS BETWEEN STRIPE LASER AND VCSEL

Parameter	Symbol	Stripe Laser	Surface Emitting Laser
Active layer Thickness	d	100Å-0.1μm	80Å-0.5μm
Active Layer Area	S	$3\times300\mu m^2$	$5\times5\ \mu m^2$
Active Volume	V	$60\mu m^3$	$0.07\ \mu m^3$
Cavity Length	L	300μm	≈1μm
Reflectivity	R_m	0.3	0.99-0.999
Optical Confinement	ξ	≈3%	≈4%
Optical Confinement (Transverse)	ξ_t	3-5%	50-80%
Optical Confinement (Longitudinal)	ξ_l	50%	2×1%×3 (3QW's)
Photon Lifetime	τ_p	≈1 ps	≈1 ps
Relaxation Frequency (Low Current Levels)	f_r	<5GHz	>10GHz

ometry lasers in Table II. Notice that the volume of VCSELs could be $V = 0.06\ \mu m^3$, whereas the stripe lasers remain $V = 60\ \mu m^3$. This directly reflects the threshold current: the typical threshold of stripe lasers ranges from microampere or higher, while that for VCSEL is less than microampere due to a simple carrier confinement scheme, such as proton bombardment. It could even be as low as microampere by implementing sophisticated carrier and optical confinement structures, as will be introduced later.

An early stage estimation of threshold showed that the threshold current can be reduced in proportion to the square of the active region diameter. However, there should be a minimum value originating from the decrease of optical confinement factor that is defined by the overlap of optical mode field and gain region when the diameter is becoming small. In addition, the extreme minimization of volume, in particular, in the lateral direction, is limited by the optical and carrier losses due to optical scattering, diffraction of lightwave, nonradiative carrier recombination, and other technical imperfections.

B. Output Power and Quantum Efficiency

Also, we discuss the differential quantum efficiency of the VCSEL. If we use a nonabsorbing mirror for the front reflector, the differential quantum efficiency η_d from the front mirror is expressed as

$$\eta_d = \frac{\alpha_m}{\alpha_a + \alpha_d + \alpha_m} = \eta_i \frac{(1/L)\ln(1/R_f)}{\alpha + (1/L)\ln\left(1/\sqrt{R_f R_r}\right)} \quad (4)$$

where α is the total internal loss $(=\alpha_a + \alpha_d)$ and R_f and R_r are front and rear mirror reflectivities.

The optical power output is expressed by

$$\begin{aligned} P_o &= \eta_d \eta_{\text{spon}} C E_g I, \qquad (I \le I_{\text{th}}) \\ &= \eta_d E_g (I - I_{\text{th}}) + \eta_d \eta_{\text{spon}} C E_g I_{\text{th}}, \qquad (I \ge I_{\text{th}}) \end{aligned} \quad (5)$$

where

E_g is bandgap energy;
C is spontaneous emission factor;
I is driving current.

On the other hand the power conversion efficiency η_P far above threshold is given by

$$\eta_P = \frac{P_o}{V_b I} = \eta_d \frac{E_g}{V_b}\left(1 - \frac{I_{\text{th}}}{I}\right) \quad (6)$$

where V_b is bias voltage and the spontaneous component has been neglected. In the case of surface-emitting laser, the threshold current could be very small and therefore, the power conversion efficiency can be relatively large, i.e., higher than 50%. The power conversion efficiency is sometimes called wall-plug efficiency.

The modulation bandwidth is given by

$$f_{3\,\text{dB}} = 1.55 f_r \quad (7)$$

where f_r denotes the relaxation frequency, which is expressed by the equation

$$f_r = \frac{1}{2\pi\tau_s}\sqrt{\frac{\tau_s}{\tau_p}\left(\frac{I}{I_{\text{th}}} - 1\right)}. \quad (8)$$

The photon lifetime τ_p is given by

$$\tau_p = \frac{n_{\text{eff}}/c}{\alpha + \alpha_m}. \quad (9)$$

The photon lifetime is normally in the order of psec, which can be made slightly smaller than stripe lasers. Since the threshold current can be very small in VCSELs, the relaxation frequency could be relatively higher than the stripe lasers even in low driving ranges. The threshold carrier density N_{th} can

be expressed in terms of photon lifetime, which represents the cavity loss and given by using (3) and (9);

$$N_{\rm th} = N_t + \frac{1}{(c/n_{\rm eff})} \times \frac{1}{(dg/dN)} \times \frac{1}{\xi} \times \frac{1}{\tau_p}. \qquad (10)$$

It is noted that the threshold carrier density can be small if we make the differential gain dg/dN, the confinement factor ξ, and the photon lifetime τ_p large.

C. Criteria for Confirmation of Lasing

When we face a new or ultralow threshold device to check the lasing operation, the existence of a break from the linear increase of light output versus injection current (I–L) characteristic is an easy observation. Sometimes a nonlinearity is observed in the I–L characteristic but this does not necessarily mean laser oscillation. Even with a nonlasing sample nonlinearity is owed to the "filtering effect," electron-hole plasma emission, and nonradiating floor. The methods used to confirm the laser operation of vertical cavity, for example, are as follows:

1) break or kink in (L–I) characteristic;
2) narrow spectral linewidth <1 Å;
3) difference of near field pattern (NFP) and far field pattern (FFP) between the emissions below and above the threshold;
4) linearly polarized light of the emission above the threshold.

III. Device Design and Material

A. Device Configuration

As already shown in Fig. 1(a), the structure common to most VCSELs consists of two parallel reflectors, which sandwich a thin active layer. The reflectivity necessary to reach the lasing threshold normally should be higher than 99.9%. Together with the optical cavity formation, the scheme for injecting electrons and holes effectively into a small volume of active region is necessary for the current injection device. The ultimate threshold current depends on how to make the active volume small, as introduced in the previous section, and how well the optical field can be confined within the cavity to maximize the overlap with active region. These confinement structures will be presented in the later sections.

B. Materials

We show some material choices for VCSELs in Fig. 2. We list problems below that should be considered when making VCSELs, as discussed in the previous section:

1) design of resonant cavity and mode-gain matching;
2) multilayered DBRs to realize high reflective mirrors;
3) optical losses such as Auger recombination, intervalence band absorption, scattering loss, and diffraction loss;
4) p-type doping to reduce the resistivity in p-type materials for CW and high efficiency operation (if we wish to form multilayer DBRs, this will become much more severe);
5) heat sinking for high-temperature and high-power operation;

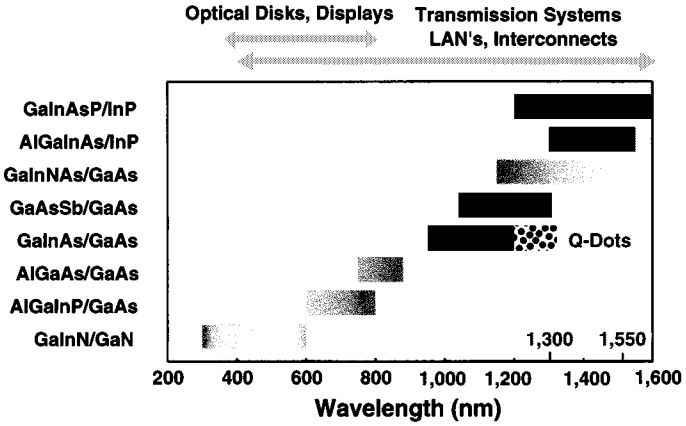

Fig. 2. Materials for VCSELs in wide spectral bands.

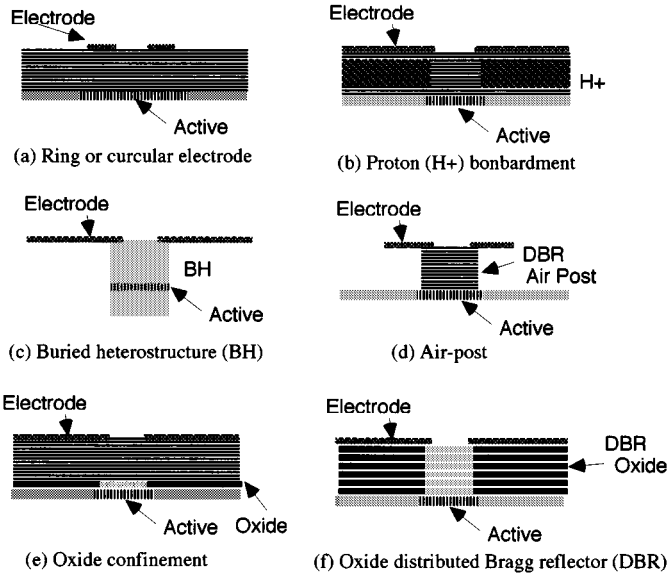

Fig. 3. Structures for current confinement.

6) catastrophic optical damage (COD) level is very important for high power operation;
7) crystal growth at reasonably high temperatures (e.g., higher than half of the melting temperatures).

C. Current Injection Scheme

Let us consider the current confinement for VCSELs. In Fig. 3, we show typical models of current confinement schemes reported so far.

a) Ring or circular electrode type: This structure can limit the current flow in the vicinity of the ring electrode. The light output can be taken out from the center window. This is easy to fabricate, but the current can not be confined completely within a small area due to diffusion.
b) Proton bombardment type: We make an insulating layer by proton (H^+) irradiation to limit the current spreading toward the surrounding area. The process is rather simple, and most of commercialized devices are made by this method.
c) Buried heterostructure (BH) type: We bury the mesa, including the active region, with a wide-gap semiconductor

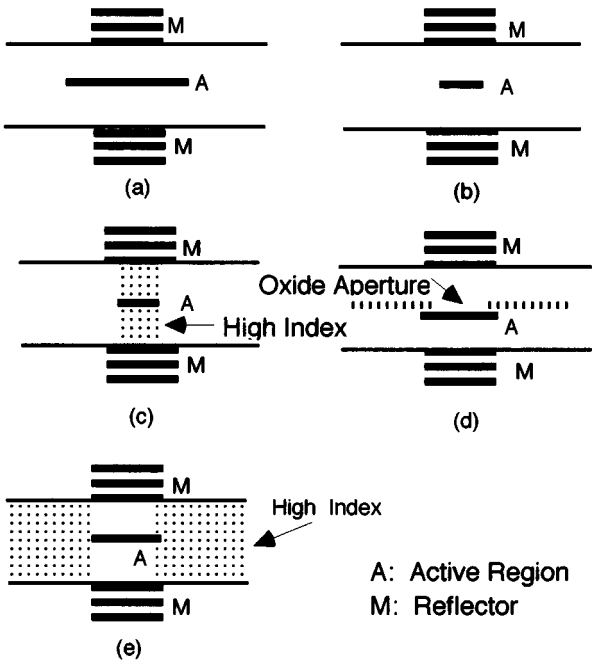

Fig. 4. Structures for optical confinement.

to limit the current. The refractive index can be small in the surrounding region, resulting in the formation of an index-guiding structure. This is an ideal structure in terms of current and optical confinement. The problem is that the necessary process is rather complicated, particularly, in making a tiny three-dimensional (3-D) device.

d) Air-post type: The circular or rectangular air-post is used to make a current confinement. This is the simplest way for device fabrication, although nonradiative recombination at the outer wall may deteriorate the performance.

e) Selective AlAs oxidation type: We oxidize the AlAs layer to make a transparent insulator.

f) Oxidized DBR type: The same method as above is applied to oxidize DBR, consisting of AlAs and GaAs. This is only one volume confinement method that can reduce the nonradiative recombination.

By developing new process technology, we could reach the laser performance, which is expected from the theoretical consideration.

D. Optical Guiding

The optical confinement schemes developed for VCSELs are introduced in Fig. 4. The fundamental concept is to increase the overlap of optical field with gain region.

a) Fabry–Perot type: The optical resonant field is determined by the two reflectors forming the plane that is parallel to the Fabry–Perot resonator. The diffraction loss increases if the mirror diameter gets too small.

b) Gain-guide type: We simply limit the field at the region where the gain exists. The mode may be changed at higher injection levels due to spatial hole burning.

c) BH: As introduced in the previous section, an ideal index guiding can be formed.

d) Selective AlAs oxidation type: Due to the index difference between AlAs and the oxidized region, we can confine the optical field as well by a lens effect.

e) Antiguiding type: The index is designed to be lower in the surrounding region in order to make a so-called antiguiding scheme. The threshold is rather high, but this structure is good for stable mode in high driving levels.

E. Transverse and Longitudinal Mode

The resonant mode in most SELs can be expressed by the well known Fabry–Perot TEM mode. The NFP of fundamental mode can be given by the Gaussian function

$$E = E_0 \exp\left[-\tfrac{1}{2}(r/s)^2\right] \tag{11}$$

where

E optical field;
r lateral distance;
s denotes spotsize.

The spotsize of normal SELs is several micronmeters, and relatively large when compared with stripe lasers, i.e., 2–3 μm. In the case of multimode operation, the mode behaves like the combination of multiple TEM$_{pq}$. The associated spectrum is broadened due to different resonant wavelengths.

FFP associated with Gaussian near field can be expressed by Gaussian function; spreading angle $\Delta\theta$ is given by

$$2\Delta\theta = 0.64(\lambda/2s). \tag{12}$$

Here, if $s = 3$ μm and $\lambda = 1$ μm, then $\Delta\theta = 0.05$ (rad) $= \cong 3°$. This kind of angle is narrower than conventional stripe lasers.

F. Polarization Mode

The VCSEL generally has linear polarization without exception. This is due to a small amount of asymmetric loss coming from the shape of the device or material. The device grown on a (100)-oriented substrate polarizes in (110) or equivalent orientations. The direction can not be identified definitely, and sometimes switches over due to spatial hole burning or temperature variation. In order to stabilize the polarization mode, special care should be taken. This issue will be discussed later.

IV. Surface-Emitting Laser in Long-Wavelength Band

A. GaInAsP–InP VCSEL

The first SEL device was demonstrated by using GaInAsP–InP system in 1978 and published in 1979 [3]. The importance of 1300- or 1550-nm devices is currently increasing because parallel lightwave systems are really needed to meet rapid increase of information transmission capacity in LANs. However, the GaInAsP–InP system, which is conventionally used in trank communication systems with the help of temperature controller, has some substantial difficulties for making VCSELs due to the following reasons.

1) Auger recombination and inter-valence band absorption (IVBA) are noticeable.
2) Index difference between GaInAsP and InP is relatively small to make DBR mirrors.
3) Conduction band offset is small.

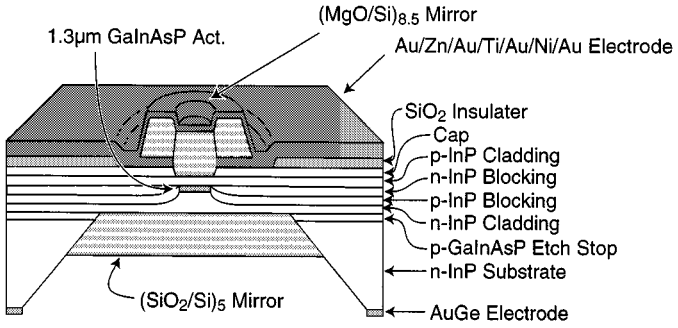

Fig. 5. 1300-nm VCSELs with thermally conductive dielectric DBR.

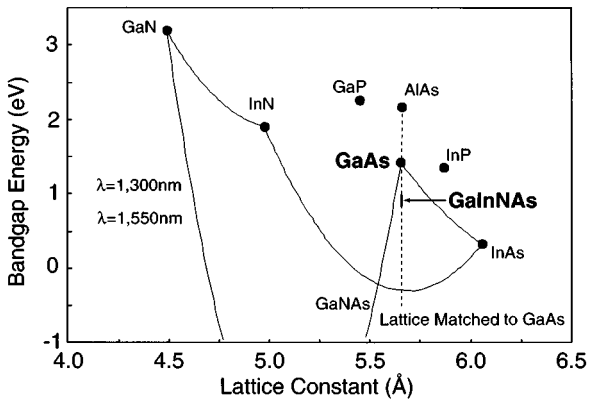

Fig. 6. Bandgap versus lattice-constant diagram.

Two hybrid mirror technologies are being developed. One uses a semiconductor/dielectric reflector [10]. Thermal problems for CW operation are extensively studied. A MgO–Si mirror with good thermal conductivity was demonstrated and achieved the first room-temperature CW operation with 1300 nm surface-emitting lasers, as shown in Fig. 5 [11]. Better results have been obtained by using Al_2O_3–Si mirrors [16].

The other is an epitaxial bonding of GaInAsP–InP active region and GaAs–AlAs mirrors, where a 144 °C pulsed operation was achieved by optical pumping. The AlAs–GaAs mirror has advantages in both electrical and thermal conductivity. CW threshold of 0.8 mA [17] and maximum operating temperature of up to 69 °C [12] have been reported for 1550-nm VCSELs with double-bonded mirrors [17]. More recently, the maximum operation was achieved at 71 °C [18]. In 1998, a tandem structure of 1300-nm VCSEL optically pumped by a 850-nm VCSEL has been demonstrated to achieve 1.5 mW of output power [19]. However, the cost of wafer consumption in wafer fusion devices may become the final bottleneck of low-cost commercialization.

Recently, a GaAsSb QW on GaAs substrate has been demonstrated for the purpose of 1300-nm VCSELs [20]. An AlGaAsSb–GaAs system has been found to form a good DBR [21]. Tunnel junction and AlAs oxide confinement structures may be very helpful for long-wavelength VCSEL innovation [22].

B. AlGaInAs–AlGaInAs VCSEL

The AlGaInAs lattice matched to InP is also considered. This system may exhibit a larger conduction band offset than the conventional GaInAsP system. Moreover, we can grow a thin AlAs layer to make the native oxide for a current confining aperture like the GaAs–AlAs system. The preliminary study has been made to demonstrate a stripe laser in our group, where a large T_0 was demonstrated. By using this system, the first monolithic VCSEL was fabricated, demonstrating room-temperature CW operation [23].

C. Long Wavelength VCSELs on GaAs Substrate

Another interesting system is GaInNAs lattice-matched to GaAs, as is shown in Fig. 6. This system has been pioneered by Kondow *et al.* [24] with a gas-source molecular-beam epitaxy (GSMBE). Also, $\lambda = 1190$-nm stripe lasers were fabricated, where the nitrogen content is 0.4%. Room-temperature CW operation of horizontal cavity lasers recently has been obtained, exhibiting the threshold current density of 1.5 kA/cm^2. Also, stripe geometry lasers were demonstrated with a threshold of 24 mA at room temperature [25]. It is reported that characteristic temperature is approximately 120K at room temperature [25]. If we can increase the nitrogen content up to 5%, the wavelength band of 1300–1550 nm may be covered. In particular, GaAs–AlAs Bragg reflectors can be incorporated on the same substrate, and AlAs oxidation is utilized [26]. Some consideration of device design was presented [27]. In any case, this system will substantially change the surface-emitting laser performances in the long wavelength range. Larson *et al.*first realized a VCSEL using this system [28].

The long-wavelength VCSEL formable on GaAs, as shown in Fig. 7 will have a great impact upon the realization of high performance devices. GaInNAs–GaAs is expected as a new material for long wavelength VCSELs. Every GaAs-based structure can be applied, and a large conduction band offset is expected. Some 1300-nm edge emitting lasers and a 1186-nm VCSELs were demonstrated. We achieved a lasing operation in GaInNAs edge emitters grown by chemical beam epitaxy (CBE), demonstrating $T_0 > 270$ K [29]. The $Ga_{1-x}In_xAs$ ternary substrate will be viable to make a high performance laser device by incorporating $\mathrm{In} = 0.25$. Some sophisticated method to form this ternary substrate is attempted, $x = 0.1$ growing [30].

During the research of GaInNAs lasers, we found that a highly strained GaInAs–GaAs system containing large In-content (≅40%) can provide an excellent temperature characteristic [31], i.e., operating with $T_0 > 200$ K [32]. This system should be viable for $\lambda > 1200$-nm VCSELs for silica-fiber-based high-speed LANs [33].

A quantum dot structure is considered as a long-wavelength active layer on a GaAs substrate. A 1150-nm GaInAs-dot VCSEL was reported with a threshold current of 0.5 mA [73].

V. Surface Emitting Laser in Midwavelength Band

A. 980-nm GaInAs–GaAs VCSEL

The GaInAs–GaAs strained pseudomorphic system grown on a GaAs substrate emitting 0.98 μm of wavelength exhibits a high laser gain and has been introduced into SELs together with GaAs–AlAs multilayer reflectors [34]. A low threshold (≅1 mA at CW) has been demonstrated by Jewell *et al.* [6]. The threshold current of VCSELs has been reduced to submilliampere orders in various institutions of the world. Very low thresholds reported

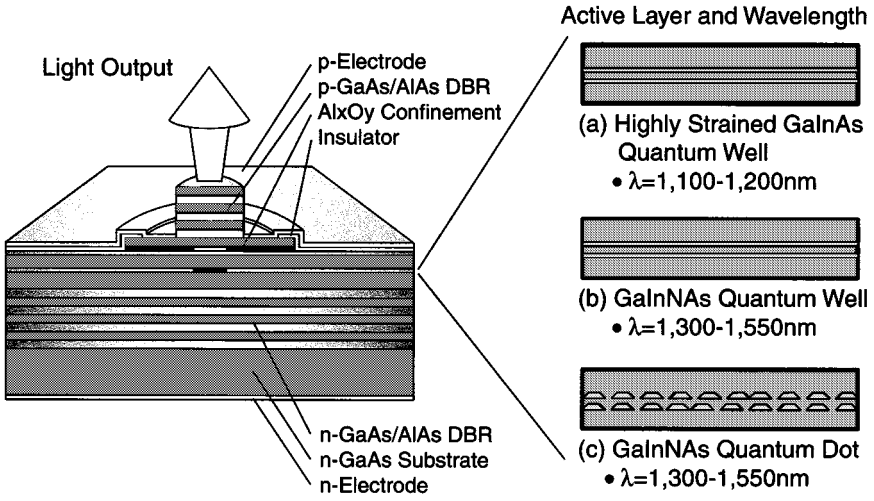

Fig. 7. Choices of long wavelength VCSELs formable on GaAs substrate.

before 1995 are 0.7 mA [7], 0.65 mA [8], and ≅0.2 mA [35]. Moreover, a threshold of 91 μA at room-temperature CW operation was reported by introducing the oxide current and optical confinement [36]. The theoretical expectation is less than 10 μA, if some good current and optical confinement structure can be introduced.

It has been made clear that the oxide aperture can function as a focusing lens since the central window has a higher index and the oxide region exhibits a lower index. This provide us with some phase shift to focus the light toward the center axis, which reduces the diffraction loss. The Al-oxide is effective both for current and optical confinements and solves the problems on surface recombination of carriers and optical scattering. We demonstrated 70 μA [37], [38] of threshold by using oxide DBR structure, 40 μA [39], and 8.5 μA [40].

In 1995, we developed a novel laser structure employing selective oxidizing process applied to AlAs, which is one member of the multilayer Bragg reflector. The schematic structure of the device now developed is shown in Fig. 8(a) [37], [38]. The active region is three quantum wells consisting of 80 Å GaInAs strained layers. The Bragg reflector consists of GaAs–AlAs quarter wavelength stacks of 24.5 pairs. After etching the epitaxial layers, including active layer and two Bragg reflectors, the sample was treated in a high-temperature oven with water vapor that had been bubbled by nitrogen gas. The AlAs layers are oxidized, preferentially with this process, and native oxide of Aluminum is formed at the periphery of etched mesas. It is recognized from SEM picture that only AlAs layers in DBR have been oxidized, as shown in Fig. 8(b) [41]. The typical size is 20-μm core starting from a 30-μm mesa diameter. We have achieved about 1 mW of power output and submicroampere threshold. The nominal lasing wavelength is 0.98 μm. We have made a smaller diameter device having 5 μm started from 20 μm mesa. The minimum threshold achieved is 70 μA at room temperature CW operation [38] as shown in Fig. 9. As the theoretically predicted, threshold is about 1 μA and this record may soon be cleared.

A relatively high power higher than 50 mW is becoming possible [42]. The power conversion efficiency 50% is reported.

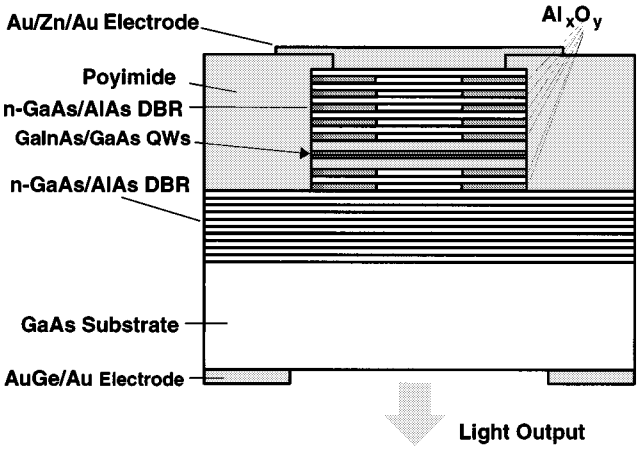

(a)

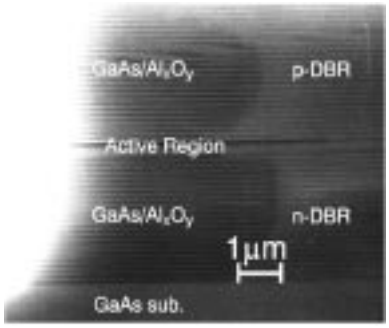

(b)

Fig. 8. (a) Schematic structure of oxide-confined GaInAs–GaAs VCSEL. (b) Oxidized AlAs layers in DBR.

[43]. Also, high efficiency operation at relatively low driving levels, i.e., a few milliamperes, became possible, which has been hard to achieve with stripe lasers. This is due to the availability of low resistive DBRs in corporation with Al-oxide aperture. In devices of about 1 μm in diameter, higher than 20% of power conversion efficiencies were reported [44], [45].

Regarding the power capability, near 200 mW has been demonstrated by a large size device in [46]. In a 2-D array involving 1000 VCSELs with active cooling, more than 2 W of CW output was achieved [47].

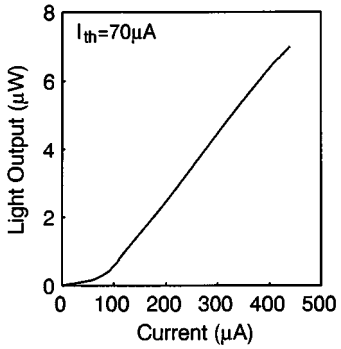

Fig. 9. Lasing characteristic showing the threshold of 70 μA.

In these low-power consumption devices, high-speed modulation is possible in low driving currents around 1 mA as well. This is substantially important in low-power interconnect applications enabling >10 Gb/s transmission or 1 Gb/s zero-bias operation [48]. Transmission experiments over 10 Gb/s and zero-bias transmission have been reported. We measured an eye diagram for 10 Gb/s transmission experiment through a 100-m multimode fiber [49].

Finally, VCSELs in this wavelength may find the market in 10 Gb LANs together with high-speed detectors and silica fibers. In any way, GaInAs VCSELs show the best performance, and the research to challenge the extreme characteristics will be continued.

B. 980-nm GaInAs–GaAs VCSEL on GaAs(311) Substrate

Most of VCSELs grown on GaAs (100) substrates show unstable polarization states due to isotropic material gain and symmetric cavity structures. VCSELs grown by MBE on GaAs (311) A substrates, however, show a very stable polarization state [50]. Also, trials of growth on (GaAs) B substrates by using MOCVD has been performed [51], [52]. Single transverse mode and polarization mode controlled VCSELs have not been realized at the same time.

In this section, we introduce a single transverse mode and polarization controlled VCSEL grown on a GaAs (311) B substrate. Both higher order transverse modes and a nonlasing orthogonal polarization modes are well suppressed with a suppression ratio of over 25 dB [53].

The schematic structure of a fabricated top-emitting VCSEL grown on GaAs (311) B is shown in Fig. 10(a), which has been grown by low pressure MOCVD [54]. The bottom n-type DBR consists of 36 pairs of $Al_{0.7}Ga_{0.3}As$–GaAs doped with Se. The top p-type DBR consists of 21 pairs of Zn-doped $Al_{0.7}Ga_{0.3}As$–GaAs and a 70-Å-thick AlAs carbon high-doping layer inserted at the upper AlGaAs interface by the carbon auto-doping technique proposed by us [41]. The active layer consists of three 8-nm-thick $In_{0.2}Ga_{0.8}As$ quantum wells and 10-nm GaAs barriers surrounded by $Al_{0.2}Ga_{0.8}As$ to form a cavity. An 80-nm-thick AlAs was introduced on the upper cavity spacer layer to form an oxide confinement. We oxidized the AlAs layer of etched 50 μm × 50 μm mesa at 480 °C for 5 min in an N_2–H_2O atmosphere by bubbling in 80 °C water and formed an oxide aperture of 2.5 μm × 3.0 μm.

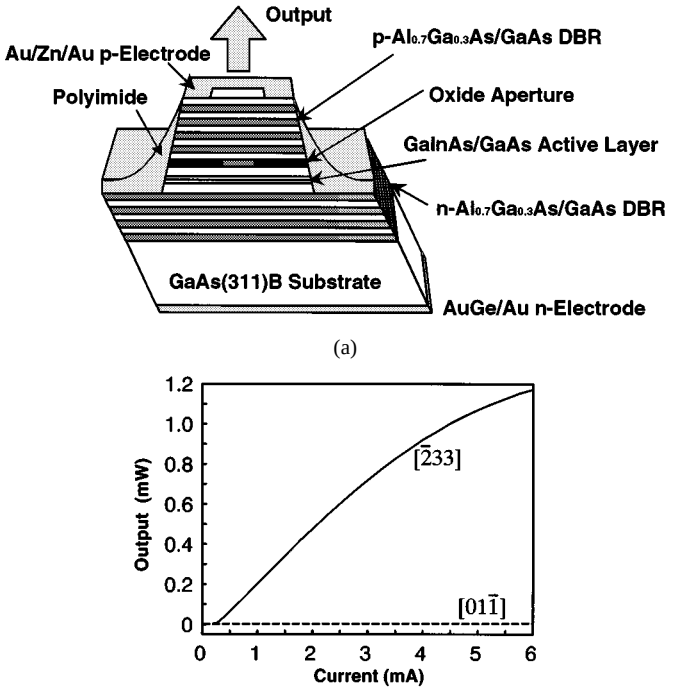

Fig. 10. InGaAs–GaAs VCSEL grown on (311) B substrate. (a) Device structure and (b) I–L characteristic exhibiting single mode and single polarization.

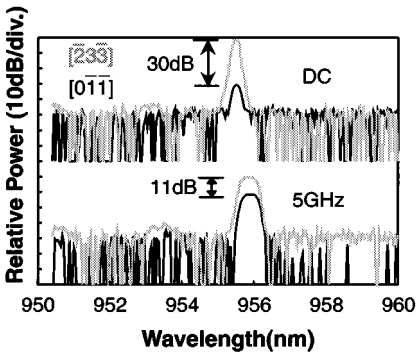

Fig. 11. Spectra of an oxide-confined InGaAs–GaAs VCSEL formed on (311) B substrate for dc and 5-Gb/s modulation conditions.

Fig. 10(b) shows a typical I–L and I–V characteristic under room-temperature CW operation. The threshold current is 260 mA, which is comparable to the lowest value reported for non(100)-substrate VCSELs. The threshold voltage is 1.5 V and the maximum output power is 0.7 mW at 4 mA.

In the entire tested driving range $(I < 16I_{\rm th})$, a large side-mode suppression ratio (SMSR) of over 35 dB and an orthogonal polarization suppression ratio (OPSR) of over 25 dB were achieved at the same time. The single polarization operation was maintained at 5-GHz modulation condition [55], [56], as shown in Fig. 11.

The selective oxidation of AlAs is becoming a standard current and optical confinement scheme for milliampere threshold devices. The technology for mode-stable lasers using (311) B substrate is demonstrated for polarization control [56]. We have

obtained completely single-mode VCSEL by employing most of the available advanced techniques.

VI. Surface-Emitting Lasers in Near Infrared-Red Band

A. 850-nm GaAlAs–GaAs VCSEL

A GaAlAs–GaAs laser can employ almost the same circular buried hetero (CBH) structure as the GaInAsP–InP laser. In order to decrease the threshold, the active region is also constricted by the selective meltback method. In 1986, a threshold of 6 mA was demonstrated for the active region diameter $\sim 6\ \mu$m under pulsed operation at 20.5 °C [4]. The threshold current density is about $J_{\rm th} \cong 200\ \mu{\rm A}/\mu{\rm m}^2$. It is noted that a microcavity of 7 μm long and 6 μm in diameter was realized.

The MOCVD grown CBH VCSEL was demonstrated by a two-step MOCVD growth and fully monolithic technology [57]. The first room-temperature CW operation was achieved in [5]. The lowest CW threshold current was 20 mA ($J_{\rm th} \cong 260\ \mu{\rm A}/\mu{\rm m}^2$). The differential quantum efficiency is typically 10%. The maximum CW output power is about 2 mW. The saturation of the output power is due to a temperature increase of the device. Stable single-mode operation is observed with neither subtransverse modes nor other longitudinal modes. The spectral linewidth above the threshold is less than 1 Å, which is limited by the resolution of the spectrometer. The mode spacing of this device was 170 Å. The side-mode suppression ratio (SMSR) of 35 dB is obtained at $I/I_{\rm th} = 1.25$. This is comparable to that of well designed DBR- or DFB-dynamic single-mode lasers.

Submilliampere thresholds and 10-mW outputs have been achieved. The power conversion efficiency of 57% has been demonstrated in [58]. Some commercial optical links have already been in markets. The price of low-skew multimode fiber ribbons may be a key issue for inexpensive multimode fiber-based data links.

As for the reliability of VCSELs, 10^7 hours of room-temperature operation is estimated, based upon the acceleration test at high temperature using proton-defined device [59]. In 1998, some preliminary test results were reported on oxide-defined devices, exhibiting no substantial negative failures.

B. 780-nm GaAlAs–GaAs VCSEL

The VCSEL in this wavelength was demonstrated in 1987 by optical pumping, and the first current injection device was developed by [9]. If we choose the Al content x to be 0.14 for $Ga_{1-x}Al_xAs$, the wavelength can be as short as 780 nm. This is common for compact disc lasers. When the quantum-well is used for active layer, blue shift should be taken into account.

We show the design below [60]. The active layer $Ga_{0.86}Al_{0.14}As$ is formed by a super lattice consisting of GaAs (33.9 Å), and AlAs (5.7 Å), with 14 period. The DBR is made of AlAs–$Al_{0.35}Ga_{0.65}As$–$Al_{0.3}Ga_{0.7}As$–$Al_{0.35}Ga_{0.65}As$ as 1 period. The n-DBR has 28.5 pair and p-DBR consists of 22 pairs. The threshold in 1991 was 4–5 mA and the output was 0.7–0.8 mW. Later on, the multiquantum wells (MQW) made of Al content $(x = 0.1/0.3)$ was introduced, and the threshold of 200 μA and the output of 1.1 mW were demonstrated [60].

C. AlGaInP Red VCSEL

Generally, the light-emitting device in short wavelength regions may have more severe operation problems than longer wavelength regions since the photon energy is large and p-type doping is technically harder to perform. If aluminum is included in the system, the degradation due to Al-oxidation is appreciable. The AlGaInP–GaAs system, emitting red color ranging from 630–670 nm, is considered a laser for the first generation digital video disc system. GaInAlP–GaAs VCSELs are developed; room-temperature operation exhibiting submilliampere threshold, 8 mW output, and 11% conversion efficiency have been obtained [59]. The wavelength is 6720 nm with oxide aperture of $2\ \mu{\rm m} \times 3\ \mu{\rm m}$. The threshold is 0.38 mA, the output is 0.6 mW, and the maximum operation temperature is 85 °C [12]. In 1998, submilliampere thresholds, 11% power conversion efficiency, 8 mW of output power were achieved [61].

VII. Surface-Emitting Lasers in Green–Blue UV Band

Visible SELs are extremely important for disk, printers, and display applications. In particular, red, green, and blue surface emitters may provide much wider technical applications, if realized. The ZnSe system is the material to provide CW operation of green-blue semiconductor lasers that operate over 1000 hours. It is supposed to be good for green lasers, and the MOCVD may be a key for getting reliable devices in mass production. We have developed a simple technique to get a high p-doping by an ampule diffusion of LiN to ZnSe. Also, a dielectric mirror deposition was investigated, and relatively high reflectivity was obtained to provide an optical pumped vertical cavity. Some trials regarding optical pumped and current-injection surface-emitting lasers have been made [14].

GaN and related materials can cover wide spectral ranges green to UV. The reported reliability of GaN-based LEDs and LDs [62], [63] seems to indicate a good material potentiality for SELs as well.

Optical gain is one of the important parameters to estimate the threshold current density of GaN-based VCSELs [64]. The estimation of linear gain for GaN–$Al_{0.1}Ga_{0.9}N$ quantum well is carried out using the density-matrix theory with intraband broadening. The transparent carrier density of GaN is higher than other III–V materials like as GaAs, presumably originating from its heavy electron and hole masses. Generally, the effective masses of electrons and holes depend on the bandgap energy. Thus, it seems that the wide-bandgap semiconductors require higher transparent carrier densities than narrow-bandgap materials. The introduction of quantum wells for wide-bandgap lasers is very effective. This result indicates that the GaN–$Al_{0.1}Ga_{0.9}N$ quantum well is useful for low threshold operation of VCSELs [65].

The trial for realizing green to UV VCSELs has just began. Some optical pumping experiments have been reported [14], [15]. It is necessary to establish some process technologies for device fabrication, such as etching, surface passivation, substrate preparation, metallization, current confinement formation, and so on [65]. We have made a preliminary study to search for dry etch of a GaN system by a chlorine-based reactive ion beam etch, which was found to be possible.

The GaN system has large potentialities for short wavelength lasers. AlN–GaN DBR and ZrO–SiO_2 DBR are formed for VCSELs [64], and some selective growth techniques have been attempted. A photo-pumped GaInN VCSEL was reported [15]. Also, we are trying to grow GaInN–GaN on silica glass for large-area light emitters [66].

VIII. Innovating Technologies

A. Targeting Characteristics

By overcoming any technical problems, such as making tiny structures, ohmic resistance of electrodes, and improving heat sinking, we believe that we can obtain a 1-μA device. A lot of effort toward improving the characteristics of SELs have been made, including surface passivation in the regrowth process for BH, microfabrication, and fine epitaxies.

As introduced before, very low thresholds of around 70, 40, and about 10 μA were reported by employing the aforementioned oxidation techniques. Therefore, by optimizing the device structures, we can expect a threshold lower than microamperes in the future [67].

The efficiency of devices is another important issue for various applications. By introducing the oxide confinement scheme, power conversion efficiency has been drastically improved due to the effective current confinement and the reduction of optical losses. Also, the reduction of driving voltage by innovating the contacting technology helped a lot. As introduced earlier, higher than 57% of power conversion efficiency, sometimes called wall-plug efficiency, has been realized. A noticeable difference of the conventional stripe laser is that high efficiency can be obtained at relatively low driving ranges in the case of VCSELs. Therefore, further improvement may enable us to achieve highly efficient arrayed devices, which have not been attained in any other type of lasers.

The high-speed modulation capability is very essential for communication applications. In VCSELs, 10-Gb/s or higher modulation experiments have been reported. For VCSEL systems, it is a great advantage that over 10-Gb/s modulation is possible at around 1-mA driving levels. This characteristic is preferable for low-power consumption optical interconnect applications [68].

The final screening for applicability of any component and system is reliability of devices. A high-temperature acceleration life test of proton-implanted VCSELs showed an expected room-temperature lifetime of over 10^7 hours [59]. There is no reason why we can not have very long-life devices by VCSELs, since the active region is completely embedded in wide-gap semiconductor materials and the mirror is already passivated.

The lasing performance of VCSELs will be improved by optimizing and solving the following issues: 1) improvement of crystal quality; 2) quantum structures (strain, wire/dot, modulation doping); 3) polarization control; 4) wavelength control; and 5) high-power and low-operation voltage.

Microetching technology is inevitable for making reproducible arrayed VCSELs. We have prepared ICP (inductively coupled plasma) etching for well-controlled and low-damage etch of GaAs and InP systems [69].

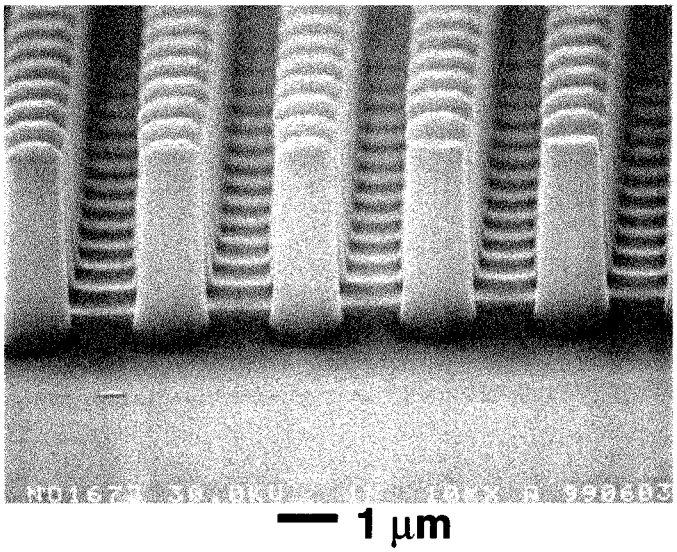

Fig. 12. SEM picture of InP microstructure by ICP etching.

An example of scanning electron microscope (SEM) picture of an etched InP system for microcavity structure is shown in Fig. 12. In order to further achieve substantial innovations in SEL performances, the following technical issues remain unsolved or nonoptimized:

1) AlAs oxidation and its application to current confinement and optical beam focusing [70], [71];
2) Modulation doping, p-type, and n-type modulation doping to quantum wells/barriers;
3) Quantum wires and dots for active engines [72], [73];
4) Strained quantum wells and strain compensation;
5) Angled substrates, such as (311A), (311B), (411);
6) New material combinations such as GaInNAs–GaAs for long wavelength emission;
7) Wafer-fusion technique to achieve optimum combination of active region and mirrors;
8) Transparent mirrors to increase quantum efficiency and output power;
9) Multiquantum barriers to prevent carrier leakage to p-cladding layer;
10) Tunnel junction.

Among them, the AlAs oxidation technology seems to be the most important technology to confine the current to reduce the threshold. Moreover, the oxidized layer works to give some amount of phase shift to focus the beam providing index guiding cavity.

A tunnel junction was introduced in SELs [74]. Recently, the reverse tunnel junction began to be utilized for effective carrier injection [22] and a noble self-aligned current aperture was proposed, as shown in Fig. 13 [22].

B. Polarization Steering

A wide variety of functions, such as polarization control, amplification, and detection, can be integrated along with SELs by stacking. The polarization control will become very important for VCSELs [75]. One method incorporates a grating terminator to a DBR. The other method includes the utilization of

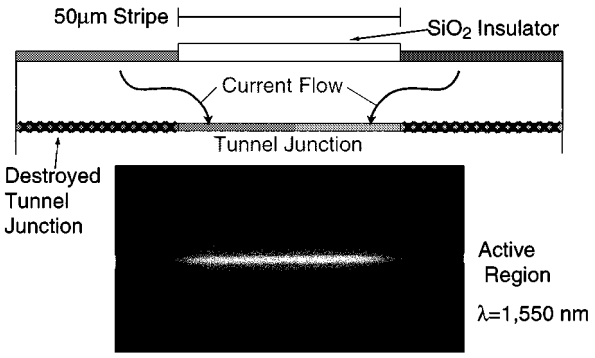

Fig. 13. Scheme of parallel fiber-optic module based on surface-emitting laser array.

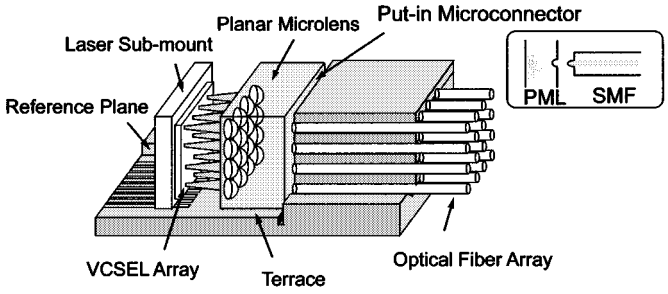

Fig. 14. MOB concept to ease the assembling of components without precise alignment.

quantum wires [72] and off-angled substrate, where we can differentiate the optical gain between one lateral direction and the perpendicular direction [50]. As already introduced, reasonably low threshold and well controlled polarization behaviors have been demonstrated by (311)A and (311)B substrates. The device formation on (311)B GaAs substrates employing MOCVD methods has been attempted by solving the difficulties of crystal growth and p-type doping. We have achieved 260 μA of CW threshold, single transverse, and single polarization operation. OPSR of about 30 dB was obtained. In Fig. 11 we show the spectra of a (311) B-based InGaAs–GaAs VCSEL under dc and a 5-Gb/s modulation condition [56]. At a high-speed modulation condition, some deterioration of OPSR was observed. The physical understanding is not clear at this moment and is open to question. In any way, the use of angled substrates, which provide us with differential gain in two orthogonal polarizations, will be very effective for controlling the polarization independent of structures and the size of devices.

IX. VCSEL-Based Integration Technology

A wide variety of functions, such as frequency tuning, amplification, and filtering, can be integrated along with SELs by stacking. Another possible way of moduling is to use the micro-optical bench concept [76] to ease the assembling of components without precise alignment, as shown in Fig. 14. Moreover, a 2-D parallel optical-logic system can deal with a large amount of image information with high speed. To this demand, an SEL will be a key device. Optical neural chips have been investigated for the purpose of making optical neurocomputers and vertical to surface transmission electro-photonic (VSTEP) integrated device [77].

High power capabilities from VCSELs are very interesting because they feature largely extending 2-D arrays. For the purpose of realizing coherent arrays, a coherent coupling of these arrayed lasers has been tried by using a Talbot cavity and considering phase compensation. It is pointed out that 2-D arrays are more suitable to make a coherent array than a linear configuration since we can take the advantage of 2-D symmetry. The research activity is now forwarded to monolithic integration of VCSELs, taking the advantage of small-cavity dimensions. A densely packed array has also been demonstrated for the purpose of making high-power lasers and coherent arrays.

Also, there are now attempts to integrate surface-operating photonic elements using quantum wells, such as an optical switch, frequency tuner, optical filter, and super-lattice functional devices. Monolithic lenses can be formed on VCSELs by an etching process to narrow the beam divergence [78].

X. VCSEL Applications

Lastly, we consider some possible applications, including optical interconnects, parallel fiber-optic subsystems, etc. We summarized possible application areas of VCSELs in Table III.

We performed an experiment of $>$10-Gb/s modulation of VCSELs and transmission via 100-m multimode fibers. The BER is shown in Fig. 15 [79]. Long-wavelength VCSELs should be useful for silica-based fiber links that provide ultimate transmission capability by taking advantage of single-wavelength operation and massively parallel integration. The development of 1200–1550-nm VCSELs may be one of the most important issues in SEL research [79].

The red-color VCSEL emitting 650 nm can match the low-loss band of plastic fibers. Short-distance data links are considered by using 1-mm diameter plastic fibers with a developed graded index. This system provides us with very easy optical coupling, and VCSELs can very nicely match this application.

By taking advantage of wide-band and small-volume transmission capability, the optical interconnect is considered to be inevitable in computer technology. A parallel interconnect scheme is wanted and new concepts are being researched. Vertical optical interconnect of LSI chips and circuit boards may be another interesting issue. New architecture for a 64-channel interconnect has been proposed and a modeling experiment was performed using GaInAs VCSEL arrays [80].

Several schemes for optical computing have been considered, but one of the bottlenecks may be a lack of suitable optical devices, in particular, 2-D VCSELs and surface-operating switches. Fortunately, very low threshold VCSELs have been developed, and stack integration together with 2-D photonic devices are now considered.

Green to UV VCSELs will be useful in the optoelectronics field as in ultra-high density optical memories. We proposed a model of optical pickup [81] using VCSEL in Fig. 16. This kind of simple pickup is now commercialized. A near-field optics scheme is considered to realize high-density optical memories [82]. In Fig. 17, a possible device was demonstrated [83], which

TABLE III
APPLICATIONS OF VCSELS

Technical Fields	Systems
1. Optical Communications	LANs, Optical links, Mobile links, etc.
2. Computer Optics	Computer links, Optical interconnects, High speed/Parallel data transfer, etc.
3. Optical Memory	CD, DVD, Near field, Multi-beam, Initializer, etc.
4. Optoelectronic Equipments	Printer, Laser pointer, Mobile tools, Home appliances, etc.
5. Optical Information Processing	Optical processors, Parallel processing, etc.
6. Optical Sensing	Optical fiber sensing, Bar code readers, Encoders, etc.
7. Displays	Array light sources, Multi-beam search-lights,
8. Illuminations	High efficiency sources, Micro illuminators, , etc. Adjustable illuminations, etc.

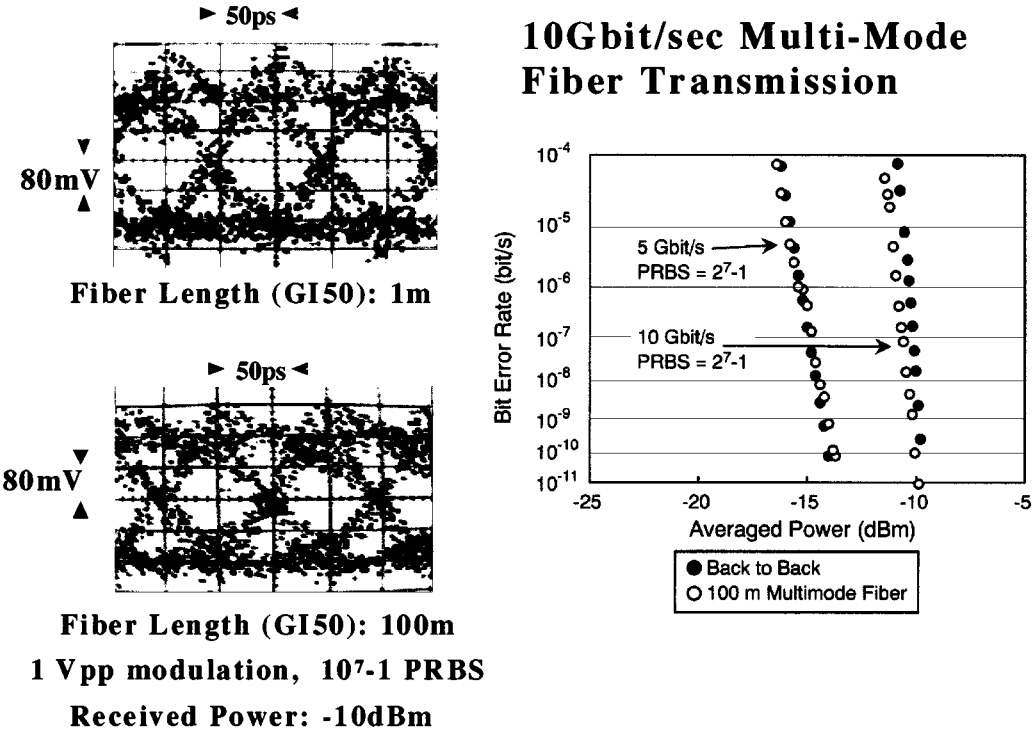

Fig. 15. BER of high-speed modulation of VCSELs transmitted via 100-m-long multimode fibers.

is useful for full-color flat displays and large-area projectors, illuminations and light signals, light decorations, UV lithography, laser processes, medical treatment, etc.

XI. SUMMARY

The technology for SELs has been developed and high-performance devices have began to be realized. Threshold current below 10–100 μA was demonstrated and extremely low thresholds lower than 1 μA are the target of research. Reasonably high-power >200 mW and power-conversion efficiency >57% are also demonstrated, which are equivalent to or better than conventional stripe lasers.

Long-wavelength devices are facing some difficulties with high temperature and large output, but there are several innovating technologies to open up the bottlenecks. Very short-wavelength lasers may cultivate wider applications if realized. The SEL is now considered a key component in ultra-low-power consumption and high-power applications over any other semiconductor laser.

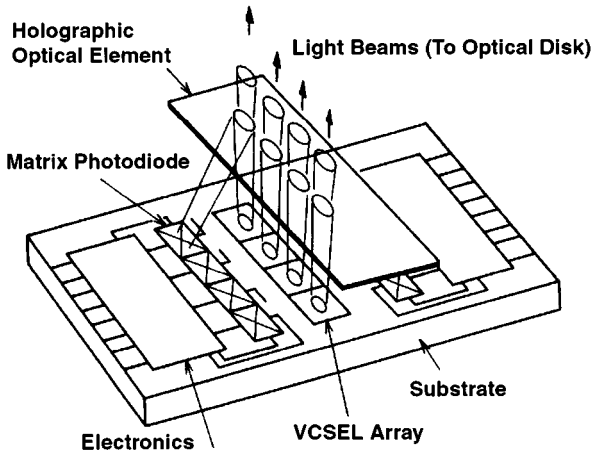

Fig. 16. Idea of optical pickup using surface-emitting laser.

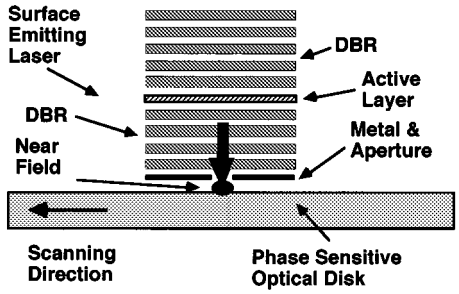

Fig. 17. VCSEL for the generation of optical near field using nano-aperture.

Vertical optical interconnects of LSI chips and circuit boards and multiple fiber systems may be the most interesting field related to VCSELs. From this point of view, the device should be as small as possible. The future process technology for it, including epitaxy and etching, will drastically change the situation of VCSELs. Some optical technologies are already introduced in various subsystems and, in addition, the arrayed microoptic technology would be very helpful for advanced systems.

The most promising application will be gigabit LANs. GaAs VCSELs emitting 850 nm of standardized wavelength are mass produced for $>$1–Gb/s LAN and simple optical links. For high-end systems, 1300–1550-nm devices are requested. By using VCSEL and micromachining technology, we demonstrated a temperature-insensitive surface normal Fabry–Perot filter for add–drop filtering in WDM. To establish an appropriate module technology utilizing VCSELs, an MOB has been investigated together with planar microlens array. Related to planar microlens array application and ultra-parallel information processing, an image recognition system is investigated using synthetic discriminant function (SDF) filtering.

In summary, the ultra-parallel optoelectronics based upon arrayed devices, including VCSELs, will open up a new era for the 2000 millennium.

ACKNOWLEDGMENT

The author would like to thank Prof. F. Koyama, T. Miyamoto, and other laboratory members for their collaboration and assistance in preparing the original drawings.

REFERENCES

[1] K. Iga, F. Koyama, and S. Kinoshita, "Surface emitting semiconductor laser," *IEEE J. Quant. Electron.*, vol. 24, pp. 1845–1855, Sept. 1988.

[2] K. Iga, "Surface emitting laser," *Trans. IEICE, C-I*, vol. JBl-C-1, no. 9, pp. 483–493, Sept. 1998.

[3] H. Soda, K. Iga, C. Kitahara, and Y. Suematsu, "GaInAsP/InP surface emitting injection lasers," *Jpn. J. Appl. Phys.*, vol. 18, pp. 2329–2330, Dec. 1979.

[4] K. Iga, S. Kinoshita, and F. Koyama, "Microcavity GaAlAs/GaAs surface-emitting laser with $I_{\rm th} = 6$ mA," *Electron. Lett.*, vol. 23, no. 3, pp. 134–136, Jan. 1987.

[5] F. Koyama, S. Kinoshita, and K. Iga, "Room-temperature continuous wave lasing characteristics of GaAs vertical cavity surface-emitting laser," *Appl. Phys. Lett.*, vol. 55, no. 3, pp. 221–222, July 1989.

[6] J. L. Jewell, S. L. McCall, A. Scherer, H. H. Houh, N. A. Whitaker, A. C. Gossard, and J. H. English, "Transverse modes, waveguide dispersion and 30-ps recovery in submicron GaAs/AlAs microresonators," *Appl. Phys. Lett.*, vol. 55, pp. 22–24, July 1989.

[7] R. Geels and L. A. Coldren, "Narrow-linewidth, low threshold vertical-cavity surface-emitting lasers," in *12th IEEE Int. Semiconductor Laser Conf.*, vol. B-1, 1990, pp. 16–17.

[8] T. Wipiejewski, K. Panzlaf, E. Zeeb, and K. J. Ebeling, "Submilliamp vertical cavity laser diode structure with 2.2-nm continuous tuning," in *18th European Conf. Opt. Comm. '92*, Sept. 1992, PDII-4.

[9] Y. H. Lee, B. Tell, K. F. Brown-Goebeler, R. E. Leibenguth, and V. D. Mattera, "Deep-red continuous wave top-surface-emitting vertical-cavity AlGaAs superlattice lasers," *IEEE Photon. Technol. Lett.*, vol. 3, no. 2, pp. 108–109, Feb. 1991.

[10] T. Miyamoto, T. Uchida, N. Yokouchi, Y. Inaba, F. Koyama, and K. Iga, "A study on gain-resonance matching of CBE grown $l = 1.5$ μm surface emitting lasers," *IEEE/LEOS Annu.*, no. DLTA13.2, p. 542, Nov. 1992.

[11] T. Baba, Y. Yogo, K. Suzuki, F. Koyama, and K. Iga, "Near room temperature continuous wave lasing characteristics of GaInAsP/InP surface emitting laser," *Electron. Lett.*, vol. 29, no. 10, pp. 913–914, May 1993.

[12] D. I. Babic, K. Streubel, R. P. Mirin, J. Pirek, N. M. Margalit, J. E. Bowers, E. L. Hu, D. E. Mars, L. Yang, and K. Carey, "Room temperature performance of double-fused 1.54 μm vertical-cavity lasers," in *IPRM 96*, Apr. 1996, no. ThA1-2.

[13] K. D. Choquette, R. P. Schneider, M. H. Crawford, K. M. Geib, and J. J. Figiel, "Continuous wave operation of 640–660 nm selectively oxidised AlGaInP vertical cavity lasers," *Electron. Lett.*, vol. 31, pp. 1145–1146, July 1995.

[14] K. Iga, "Possibility of Green/Blue/UV surface emitting lasers," in *Int. Symp. Blue Laser Light Emitting Diodes*, Mar. 1996, Th-11, pp. 263–266.

[15] T. Someya, K. Tachibana, Y. Arakawa, J. Lee, and T. Kamiya, "Lasing oscillation in InGaN vertical cavity surface emitting lasers," in *16th Int. Semiconductor Laser Conf.*, 1998, PD-1, pp. 1–2.

[16] S. Uchiyama, N. Yokouchi, and T. Ninomiya, "Room-temperature CW operation of 1.3-μm GaInAsP SL-MQW surface emitting laser," in *43th Spring Meeting Jpn. Soc. Appl. Phys.*, 1996, 26p-C-7.

[17] N. M. Margalit, D. I. Babic, K. Streubel, R. P. Mirin, R. L. Naone, J. E. Bowers, and E. L. Hu, "Submilliamp long wavelength vertical cavity lasers," *Electron. Lett.*, vol. 32, p. 1675, Aug. 1996.

[18] K. A. Black, N. M. Margalit, E. R. Hegblom, P. Abraham, Y.-J. Chiu, J. Piprek, J. E. Bowers, and E. L. Hu, "Double-fused 1.5 μm vertical cavity lasers operating continuous wave up to 71 °C," in *16th Int. Semiconductor Laser Conf.*, 1998, ThA8, pp. 247–248.

[19] V. Jayaraman, J. C. Geske, M. H. MacDougal, F. H. Peters, T. D. Lowes, and T. T. Char, "Uniform threshold current, continuous-wave, single mode 1300 nm vertical cavity lasers from 0 to 70 °C," *Electron. Lett.*, vol. 34, no. 14, pp. 1405–1407, July 1998.

[20] M. Yamada, T. Anan, K. Kurihara, K. Nishi, K. Tokutome, A. Kamei, and S. Sugou, "Room temperature low threshold CW operation of 1.23 μm GaAsSb VCSELs of GaAs substrates," *Electron. Lett.*, vol. 36, no. 7, pp. 637–638, Mar. 2000.

[21] E. Hall, G. Almuneau, J. K. Kim, O. Sjölund, H. Kroemer, and L. A. Coldren, "Electrically-pumped, single-epitaxial VCSELs at 1.55 μm with Sb-based mirrors," *Electron. Lett.*, vol. 35, no. 16, pp. 1337–1338, Aug. 1999.

[22] S. Sekiguchi, T. Miyamoto, T. Kimura, F. Koyama, and K. Iga, "Self-arraigned current confinement structure using AlAs/InP tunnel junction in GaInAsP/InP semiconductor lasers," *Appl. Phys. Lett.*, vol. 75, no. 11, pp. 1512–1514, Sep. 1999.

[23] C. Kazmierski, J. P. Debray, R. Madani, N. Bouadma, J. Etrillard, I. Sagnes, F. Alexandre, and M. Quillec, "First all-monolithic VCSELs on InP : $+55$ °C pulse lasing at 1.56 μm with GaInAlAs/InP system," in *16th Int. Semiconductor Laser Conf.*, 1998, PD-3, pp. 5–6.

[24] M. Kondow, K. Nakahara, T. Kitatani, Y. Yazawa, and K. Uomi, "GaInNAs laser diode pulsed operation at 77 K," in *OECC'96*, 18D-3-2.

[25] K. Nakahara, M. Kondow, T. Kitatani, M. C. Larson, and K. Uomi, "1.3-μm continuous-wave lasing operation in GaInNAs quantum-well lasers," *IEEE Photon. Technol. Lett.*, vol. 10, pp. 487–488, Apr. 1998.

[26] K. Iga, "Vertical cavity surface emitting lasers based on InP and related compounds—Bottleneck and corkscrew," in *Conf. Indium Phosphide Related Materials*, Schwabisch Gmund, Germany, Apr. 1996.

[27] T. Miyamoto, K. Takeuchi, F. Koyama, and K. Iga, "Novel GaInNAs/GaAs quantum well structure for long wavelength semiconductor lasers," *IEEE Photon. Technol. Lett.*, vol. 9, pp. 1448–1450, Nov. 1997.

[28] M. C. Larson, M. Kondow, T. Kitatani, K. Nakahara, K. Tamura, H. Inoue, and K. Uomi, "Room-temperature pulsed operation of GaInNAs/GaAs long-wavelength vertical cavity lasers," in *IEEE/LEOS'97*, Nov. 1997, no. PD1.3.

[29] T. Kageyama, T. Miyamoto, S. Makino, N. Nishiyama, F. Koyama, and K. Iga, "High-temperature operation up to 170 °C of GaInNAs–GaAs quantum-well lasers grown by chemical beam epitaxy," *IEEE Photon. Technol. Lett.*, vol. 12, pp. 10–12, Jan. 2000.

[30] H. Ishikawa, K. Otsubo, and H. Imai, "Experimental and theoretical analysis of the temperature performance of high T_0 lasers on InGaAs ternary substrate," in *16th IEEE Int. Semiconductor laser Conf.*, Oct. 1998, TuE51, pp. 195–196.

[31] D. Schlenker, T. Miyamoto, Z. Chen, F. Koyama, and K. Iga, "1.17 μm highly strained GaInAs–GaAs quantum-well laser," *IEEE Photon. Technol. Lett.*, vol. 11, pp. 946–948, Aug. 1999.

[32] Z. Chen, D. Schlenker, T. Miyamoto, T. Kondo, M. Kawaguchi, F. Koyama, and K. Iga, "High-temperature characteristics of near 1.2 μm InGaAs/AlGaAs lasers," *Jpn. J. Appl. Phys.*, vol. 38, no. 10B, pp. L1178–1179, Oct. 1999.

[33] F. Koyama, S. Schlenker, T. Miyamoto, Z. Chen, A. Matsutani, T. Sakaguchi, and K. Iga, "1.2 μm highly strained GaInAs/GaAs quantum-well lasers for single-mode fibre datalink," *Electron. Lett.*, vol. 35, no. 13, pp. 1079–1081, June 1999.

[34] T. Sakaguchi, F. Koyama, and K. Iga, "Vertical cavity surface emitting laser with and AlGaAs/AlAs Bragg reflector," *Electron. Lett.*, vol. 24, no. 15, pp. 928–929, July 1988.

[35] T. Numai, T. Kawakami, T. Yoshikawa, M. Sugimoto, Y. Sugimoto, H. Yokoyama, K. Kasahara, and K. Asakawa, "Record low threshold current in microcavity surface-emitting laser," *Jpn. J. Appl. Phys.*, vol. 32, no. 10B, pp. L1533–L1534, Oct. 1993.

[36] D. L. Huffaker, D. G. Deppe, C. Lei, and L. A. Hodge, "Sealing AlAs against oxidative decomposition and its use in device fabrication," in *CLEO'96*, Anaheim, no. JTuH5.

[37] Y. Hayashi, T. Mukaihara, N. Hatori, N. Ohnoki, A. Matsutani, F. Koyama, and K. Iga, "Lasing characteristics of low-threshold oxide confinement InGaAs–GaAlAs vertical-cavity surface-emitting lasers," *IEEE Photon. Technol. Lett.*, vol. 7, pp. 1234–1236, Nov. 1995.

[38] ——, "Record low threshold index-guided InGaAs/GaAlAs vertical-cavity surface-emitting laser with a native oxide confinement structure," *Electron. Lett.*, vol. 31, no. 7, pp. 560–561, Mar. 1995.

[39] D. L. Huffaker, J. Shin, and D. G. Deppe, "Low threshold half-wave vertical-cavity lasers," *Electron. Lett.*, vol. 30, pp. 1946–1947, Nov. 1994.

[40] G. M. Yang, M. MacDougal, and P. D. Dupkus, "Ultralow threshold current vertical cavity surface emitting lasers obtained with selective oxidation," *Electron. Lett.*, vol. 31, pp. 886–888, May 1995.

[41] N. Hatori, A. Mizutani, N. Nishiyama, F. Motomura, F. Koyama, and K. Iga, "P-type delta doped InGaAs/GaAs quantum well vertical-cavity surface-emitting lasers," *IEICE C-I*, vol. J81-C-I, no. 7, pp. 410–416, 1998.

[42] F. H. Peters, M. G. Peters, D. B. Young, J. W. Scott, B. J. Tibeault, S. W. Corzine, and L. A. Coldren, "High power vertical cavity surface emitting lasers," in *13th IEEE Semiconductor Laser Conf.*, 1992, PD-1, pp. 1–2.

[43] K. L. Lear, R. P. Schneider Jr., K. D. Choquette, S. P. Kilcoyne, and K. M. Geib, "Selectively oxidised vertical cavity surface emitting lasers with 50% power conversion efficiency," *Electron. Lett.*, vol. 31, pp. 208–209, Feb. 1995.

[44] K. D. Choquette, A. A. Allerman, H. Q. Hou, G. R. Hadley, K. M. Geib, and B. E. Hammons, "Improved efficiency of small area selectively oxidized VCSELs," in *16th Int. Semiconductor Laser Conf.*, Oct. 1998, ThA3, pp. 237–238.

[45] L. A. Coldren, E. R. Hegblom, and N. M. Margalit, "Vertical cavity lasers with record efficiency at small sizes using tapered apertures," in *16th Int. Semiconductor Laser Conf.*, Oct. 1998, PD-2, pp. 3–4.

[46] B. Weigl, G. Reiner, M. Grabherr, and K. J. Ebeling, "High-power selectively oxidized vertical-cavity surface-emitting lasers," in *CLEO'96*, Anaheim, June 1996, JTuH2.

[47] D. Francis, H.-I. Chen, W. Yuen, G. Li, and C. Chang-Hasnain, "Monolithic 2D-VCSEL array with 0.2 W CW output power," in *16th Int. Semiconductor Laser Conf.*, Oct. 1998, TuE3, pp. 99–100.

[48] B. J. Thibeault, K. Bertilsson, E. R. Hegblom, P. D. Floyd, and L. A. Coldren, "High-speed modulation characteristics of oxide-apertured vertical-cavity lasers," in *15th IEEE Int. Semicon. Laser Conf.*, 1996, M3.2, pp. 17–18.

[49] N. Hatori, A. Mizutani, N. Nishiyama, A. Matsutani, T. Sakaguchi, F. Motomura, F. Koyama, and K. Iga, "An over 10 Gb/s transmission experiment using p-type d-doped InGaAs/GaAs quantum-well vertical cavity surface-emitting laser," *IEEE Photon. Technol. Lett.*, vol. 10, pp. 194–196, Feb. 1998.

[50] M. Takahashi, N. Egami, T. Mukaihara, F. Koyama, and K. Iga, "Lasing characteristics of GaAs (311)A substrate based InGaAs/GaAs vertical cavity surface emitting lasers," *IEEE J. Select. Topics Quantum Electron.*, vol. 3, no. 2, pp. 372–378, Apr. 1997.

[51] K. Tateno, Y. Ohiso, C. Amano, A. Wakatsuki, and T. Kurokawa, "Growth of vertical-cavity surface-emitting laser structures on GaAs (311)B substrates by metalorganic chemical vapor deposition," *Appl. Phys. Lett.*, vol. 70, no. 25, pp. 3395–3396, June 1997.

[52] A. Mizutani, N. Hatori, N. Ohnoki, N. Nishiyama, N. Ohtake, F. Koyama, and K. Iga, "P-type doped AlAs growth on GaAs (311)B substrate using carbon auto-doping for low resistance GaAs/AlAs distributed Bragg reflectors," *Jpn. J. Appl. Phys.*, vol. 36, no. 11, pp. 6728–6729, Nov. 1997.

[53] A. Mizutani, N. Hatori, N. Nishiyama, F. Koyama, and K. Iga, "A low threshold polarization-controlled vertical cavity laser grown on GaAs (311) substrate," *IEEE Photon. Technol. Lett.*, vol. 10, pp. 633–635, May 1998.

[54] N. Nishiyama, A. Mizutani, N. Hatori, F. Koyama, and K. Iga, "Single mode and stable polarization InGaAs/GaAs surface emitting laser grown on GaAs (311)B substrate," in *16th Int. Semiconductor Laser Conf.*, 1998, ThA1, pp. 233–234.

[55] ——, "Single transversemode and stable polarization operation under high-speed modulation of InGaAs/GaAs vertical cavity surface emitting laser grown on GaAs (311)B substrate," *IEEE Photon. Technol. Lett.*, vol. 10, pp. 1676–1678, Dec. 1998.

[56] N. Nishiyama, A. Mizutani, N. Hatori, M. Arai, F. Koyama, and K. Iga, "Lasing characteristics of InGaAs/GaAs polarization controlled vertical-cavity surface emitting laser grown on GaAs (311) B substrate," *Select. Topics Quantum Electron.*, vol. 5, pp. 530–536, Feb. 1999.

[57] F. Koyama, K. Tomomatsu, and K. Iga, "GaAs surface emitting lasers with circular buried heterostructure grown by metalorganic chemical vapor deposition and two-dimensional laser array," *Appl. Phys. Lett.*, vol. 52, no. 7, pp. 528–529, Feb. 1988.

[58] R. Jager, M. Grabherr, C. Jung, R. Michalzik, G. Reiner, B. Weigl, and K. J. Ebeling, "57% wallplug efficiency oxide-confined 850 nm wavelength GaAs VCSELs," *Electron. Lett.*, vol. 33, no. 4, pp. 330–331, Feb. 1997.

[59] J. K. Guenter, R. A. Hawthorne, D. N. Granville, M. K. Hibbs-Brenner, and R. A. Morgan, "Reliability of proton-implanted VCSELs for data communications," *Proc. SPIE*, vol. 2683, p. 1, 1996.

[60] H.-E. Shin, Y.-G. Ju, H.-H. Shin, J.-H. Ser, T. Kim, E.-K. Lee, I. Kim, and Y. -H. Lee, "780 nm oxidised vertical-cavity surface-emitting lasers with $Al_{0.11}Ga_{0.89}As$ quantum wells," *Electron. Lett.*, vol. 32, no. 14, pp. 1287–1288, July 1996.

[61] M. H. Crawford, K. D. Choquette, R. J. Hickman, and K. M. Geib, "Performance of selectively oxidized AlGaInP-based visible VCSELs," *OSA Trends Optics Photon. Series*, vol. 15, pp. 104–105, 1998.

[62] S. Nakamura, M. Senoh, S. Nagahama, N. Iwasa, T. Yamada, T. Matsushita, H. Kiyoku, and Y. Sugimoto, "InGaN-based multi-quantum-well-structure laser diodes," *Jpn. J. Appl. Phys.*, pt. 2, vol. 35, no. 1B, pp. L74–L76, Jan. 1996.

[63] S. Nakamura, M. Senoh, S. Nagahama, N. Iwasa, T. Yamada, T. Matsushita, H. Kiyoku, Y. Sugimoto, T. Kozaki, H. Umemoto, M. Sano, and K. Chocho, "High-power, long-lifetime InGaN/GaN/AlGAN-based laser diodes grown on pure GaN substrates," *Jpn. J. Appl. Phys.*, vol. 37, pp. L309–L312, Mar. 1998.

[64] T. Sakaguchi, T. Shirasawa, N. Mochida, A. Inoue, M. Iwata, T. Honda, F. Koyama, and K. Iga, "Highly reflective AlN/GaN and ZrO_2/SiO_2 multilayer distributed Bragg reflectors for InGaN/GaN surface emitting lasers," in *LEOS 1998 11th Annual Meeting Conf. Proc.*, TuC4, Dec. 1998.

[65] T. Shirasawa, N. Mochida, A. Inoue, T. Honda, T. Sakaguchi, F. Koyama, and K. Iga, "Interface control of GaN/AlGaN quantum well structures in MOVPE growth," *J. Cryst. Growth*, pp. 124–127, 1998.

[66] Y. Moriguchi, T. Miyamoto, T. Sakaguchi, M. Iwata, Y. Uchida, F. Koyama, and K. Iga, "GaN polycrystal growth on silica substrate by metalorganic vapor phase epitaxy (MOVPE)," in *3rd Int. Symp. Blue Laser Light Emitting Diodes*, Berlin, Mar. 2000, WeP-19, p. 83.

[67] K. Iga and F. Koyama, "Surface emitting lasers," in *Academic Monthly*, Gakujyutsu-Geppo; JSPS ed., Jan. 1996, vol. 49, no. 1, pp. 42–46.

[68] B. E. Lemoff and L. A. Buckman, "Low-cost WDM transceivers for the LAN," in *Dig. LEOS-Summer Topical Meeting*, 1999, MA2.1, pp. 3–4.

[69] A. Matsutani, H. Ohtsuki, F. Koyama, and K. Iga, "C60 resist mask of electron beam lithography for chlorine-based reactive ion beam etching," *Jpn. J. Appl. Phys.*, vol. 37, no. 7, pp. 4211–4212, July 1998.

[70] D. G. Deppe, D. L. Huffaker, J. Shin, and Q. Deng, "Very-low-threshold index-confined planar microcavity lasers," *IEEE Photon. Technol. Lett.*, vol. 7, pp. 965–967, Sept. 1995.

[71] H. Bissessur, F. Koyama, and K. Iga, "Modeling of oxide-confined vertical cavity surface emitting lasers," *IEEE J. Quantum Electron.*, vol. 3, pp. 344–352, Apr. 1997.

[72] N. Hatori, T. Mukaihara, Y. Hayashi, N. Ohnoki, F. Koyama, and K. Iga, "Design and fabrication of InGaAs/GaAs quantum wires for vertical-cavity surface-emitting lasers," *Jpn. J. Appl. Phys.*, vol. 35, no. 3, pp. 1777–1778, Mar. 1996.

[73] D. G. Deppe, D. L. Huffaker, Q. Deng, T.-H. Oh, and L. A. Graham, "Oxide-confined VCSELs with quantum well quantum dot active region," in *IEEE/LEOS'97*, Nov. 1997, no. ThA 1, pp. 287–288.
[74] Y. Kotaki, S. Uchiyama, and K. Iga, "GaInAsP/InP surface emitting laser with two active layers," in *1984 Int. Conf. Solid-State Devices*, no. C-2-3.
[75] T. Mukaihara, N. Ohnoki, Y. Hayashi, N. Hatori, F. Koyama, and K. Iga, "Polarization control of vertical-cavity surface-emitting lasers using a birefringent metal/dielectric polarizer loaded on top distributed Bragg reflector," *IEEE J. Select. Topics Quantum Electron.*, vol. 1, pp. 667–673, June 1995.
[76] Y. Aoki, R. J. Mizuno, Y. Shimada, and K. Iga, "Parallel and bi-directional optical interconnect module using vertical cavity surface emitting lasers(VCSELs) and 3-D micro optical bench (MOB)," in *1999 IEEE/LEOS Summer Topical Meetings*, July 1999, WA2.4, pp. 9–10.
[77] T. Numai, M. Sugimoto, I. Ogura, H. Kosaka, and K. Kasahara, "Current versus light-output characteristics with no definite threshold in pnpn vertical to surface transmission electro-photonic devices with a vertical cavity," *Jpn. J. Appl. Phys.*, vol. 30, no. 4A, pp. L602–L604, Apr. 1991.
[78] K. Iga, T. Kambayashi, K. Wakao, C. Kitahara, and K. Moriki, "GaInAsP/InP double-structure planar LEDs," *IEEE Trans. Electron. Devices*, vol. ED-26, pp. 1227–1230, Aug. 1979.
[79] F. Koyama, D. Schlenker, T. Miyamoto, Z. Chen, A. Matsutani, T. Sakaguchi, and K. Iga, "Data transmission over single-mode fiber by using 1.2-mm uncooled GaInAs–GaAs laser for Gb/s local area network," *IEEE Photon. Technol. Lett.*, vol. 12, pp. 125–127, Feb. 2000.
[80] H. Kosaka, M. Kajita, Y. Li, and Y. Sugimoto, "A two-dimensional optical parallel transmission using a vertical-cavity surface-emitting laser array module and an image fiber," *IEEE Photon. Technol. Lett.*, vol. 9, pp. 253–255, Feb. 1997.
[81] K. Iga, "Surface operating electrooptic devices and their application to array parallel signal processing," in *ECOC'90*, vol. 2, Sept. 1990, WeB-2.1, pp. 895–932.
[82] K. Goto, "Tera bytes optical disk with electric tracking control using micro-cavity VCSEL array and PD array," in *Dig. LEOS-Summer Topical Meeting*, 1997, MC-4, pp. 21–22.
[83] T. Yamatoya, S. Mori, F. Koyama, and K. Iga, "Design and fabrication of high power and broad-band GaInAsP/InP strained quantum well superluminescent diodes with tapered active region," in *CLEO Pacific Rim'99*, July 1999, FO6v, pp. 1227–1228.

Kenichi Iga (S'67–M'68–SM'80–F'87) was born in Hiroshima Prefecture, Japan, in 1940. He received the B.E., M.E., Dr.Eng. degrees from the Tokyo Institute of Technology, Tokyo, Japan, in 1963, 1965, and 1968, respectively.

In 1968, he joined the P & I Laboratories, Tokyo Institute of Technology, where he became an Associate Professor in 1973 and Professor in 1984. Since 1993, he has been a Teiichi Yamazaki Chair Professor. He is currently the Director of Institute Library and the Director of P & I Microsystem Research Center. From 1979 to 1980, he was with Bell Laboratories as a Visiting Technical Staff Member. He is the author of many books, including *Fundamentals of Microoptics* (New York: Academic), *Fundamentals of Laser Optics* (New York: Plenum), *Introduction to Optical Fiber Communication* (New York: Wiley), and *Process Technology for Semiconductor Lasers* (New York: Springer-Verlag). He first proposed and pioneered the research of surface-emitting semiconductor lasers, which triggered research activities in surface-emitting lasers and has become very important as coherent light-sources with two-dimensional (2-D) parallelism. His research interests include microoptics, gradient-index microlens arrays, and the realization of 2-D arrayed optical devices in combination with surface-emitting lasers.

Prof. Iga is a Member of the Institute of Electronics, Information, and Communication Engineers of Japan (IEICE) and a Fellow of the Optical Society of America. He has served as an Asian Representative for the IEEE Lasers and Electro-Optics Society (IEEE/LEOS) from 1984 to 1990, CLEO Japanese Subcommittee Chair from 1988 to 1990, Board of Governor for IEEE/LEOS from 1991 to 1993, and President of the Electronics Society in 1996. He has received numerous awards, including the Inada Memorial Prize in 1966, IEICE Distinguished Book Award for *Introduction to Optical Fiber Communications* in 1978, the Sakurai Memorial Prize from the Optoelectronic Industry and Technology Development Association in 1987, IEE Premium Award in 1988, the William Streifer Award for Scientific Achievement in 1992, the Toray Award in 1995, the IEEE Third Millennium Medal, and the John Tyndall Awardin 1998.